Carbon Monoxide Binding to *Rhodospirillum molischianum* Ferrocytochrome *c'* †

Michael L. Doyle,* Patricia C. Weber,‡ and Stanley J. Gill

Department of Chemistry, University of Colorado, Boulder, Colorado 80309

Received August 7, 1984

ABSTRACT: Reversible carbon monoxide binding has been used to examine the structural and functional properties of reduced *Rhodospirillum molishchianum* cytochrome *c'*. The symmetrical dimer is found to bind CO in a noncooperative manner, indicating that the heme sites function independently and with identical carbon monoxide affinity. The enthalpy change of binding CO (aqueous) to *R. molischianum* ferrocytochrome *c'* is determined to be −11 kcal/mol of CO, which is comparable to the heat of CO binding to other heme proteins. A Bohr effect is observed (0.31 ± 0.04 proton released per mole of CO bound at pH 8), and a basic group is involved which changes its p*K* from 8.3 to 7.8 upon ligation. The histidine axial ligand to the heme iron is suggested to be the source of the Bohr effect. Increased CO affinities were observed at high pH or at neutral pH in the presence of phosphate. These solvent-induced changes in CO affinity do not appear to be caused by changes in quaternary structure but rather are more likely brought about by localized changes in the vicinity of the solvent-exposed heme face.

Cytochromes *c'* are isolated from denitrifying and photosynthetic bacteria as dimeric, high-spin heme proteins (Bartsch, 1978). Each 14 000-dalton subunit of the dimer incorporates a single covalently bound protoheme IX prosthetic group. The covalent mode of heme attachment serves to classify these molecules as *c*-type cytochromes. The prime superscript indicates that the heme iron is high spin and also distinguishes these proteins from the structurally dissimilar low-spin mitochondrial cytochromes *c*. Of the ligands O_2, NO, CO, CN^-, N_3^-, and ethyl isocyanide, which bind to typical high-spin heme proteins, only CO and ethyl isocyanide have been found to bind reversibly to a variety of cytochromes *c'* (Cusanovich & Gibson, 1973; Taniguchi & Kamen, 1963; Rubinow & Kassner, 1984). The gaseous nature of carbon monoxide offers a unique experimental advantage in permitting high-precision binding studies by means of a thin-layer optical technique (Dolman & Gill, 1978). The linkage between carbon monoxide binding and solution ligands such as protons and phosphate can be thoroughly investigated in this manner.

The carbon monoxide affinities for several ferrocytochromes *c'* have been determined by equilibrium measurements (Cusanovich & Gibson, 1973) and are generally much lower than those for myoglobin or hemoglobin (Antonini & Brunori, 1971). The three-dimensional structure of *Rhodospirillum molischianum* cytochrome *c'* has been determined by X-ray crystallographic techniques (Weber et al., 1981). For this reason, we have chosen to study the equilibrium properties of CO binding to *R. molischianum* ferrocytochrome *c'* and to correlate these functional properties to the known structural information.

In addition to questions concerning the structural basis for the low carbon monoxide affinity, a key question concerns the functional importance of the dimeric state of this protein. One possibility is that the dimer exists to allow for allosteric control between subunits. To test this proposal, we have analyzed the equilibrium properties of carbon monoxide binding to *R. molischianum* ferrocytochrome *c'* at a high level of precision to see if allosteric changes occur. In this connection, we have also examined the effect of pH and other potential effector molecules.

Materials and Methods

Rhodospirillum molischianum cytochrome *c'* was prepared according to the method of Bartsch (1971) and then dialyzed against 0.1 M tris(hydroxymethyl)aminomethane (Tris) buffer. The pH was adjusted by addition of either hydrochloric acid or sodium hydroxide. In some cases, potassium phosphate was added to the buffer in order to study its effect on CO binding.

The enzymatic reducing system of Hayashi et al. (1973) was used to ensure complete reduction of the cytochrome sample throughout the experiment. All components of the system were products of Sigma Corp. This method of reduction is milder and more suitable for our thin-layer technique than the typically used reductant dithionite. Characteristic CO-bound and reduced cytochrome *c'* spectra were recorded prior to and after each experiment in the Soret region with a Cary 219 spectrophotometer.

A thin-layer optical cell (Dolman & Gill, 1978), holding a thin layer of cytochrome *c'* solution between a glass window and a transparent gas-permeable membrane, was used to study the CO binding reaction at a wavelength of 417 nm. The thickness of the layer was 0.002 in. and the concentration of the protein used was in the range of 0.1–0.4 mM heme. At the beginning of each experiment, the cell was filled with CO to atmospheric pressure. The partial pressure of CO was then accurately diluted through a series of "steps" with nitrogen, by means of a precision dilution valve connected to the cell. The dilution valve dilutes the partial pressure of CO by a factor of 0.705 at each stepwise dilution. Each step required about 5 min for the solution to reach equilibrium.

The experimental binding data were found to fit an expression of two equivalent independent-site reactions (see eq 3) as it relates to the measured optical density change, $\Delta OD(i)$, for the ith dilution step, where the CO partial pressure changes from $p_{CO}(i-1)$ to $p_{CO}(i)$. If the total optical density change

† This work was supported by National Institutes of Health Grant HL22325.

‡ Present address: Protein Engineering Division, Genex Corp., Gaithersberg, MD 20877.

0006-2960/85/0424-1987$01.50/0

for complete CO saturation is designated by ΔOD(total), then the stepwise change in optical density is given as

$$\Delta OD(i) = \Delta OD(\text{total})\left[\frac{\kappa_{CO}p_{CO}(i-1)}{1+\kappa_{CO}p_{CO}(i-1)} - \frac{\kappa_{CO}p_{CO}(i)}{1+\kappa_{CO}p_{CO}(i)}\right] \quad (1)$$

This expression was used to fit the data by means of the Marquardt procedure as described by Bevington (1969) in order to obtain the best fitting parameters of κ_{CO} and ΔOD(total) along with standard error estimates for a given experiment.

Since the change in optical density, ΔOD(i), is directly proportional to the difference in the fraction of CO bound between the initial and final partial pressures defining the step i, and these pressures are simply determined by the constant dilution factor of the experiment, then it follows that ΔOD(i) will give a good approximation of the slope of the binding curve, $\Delta\bar{X}/\Delta \ln p_{CO}$, for the average pressure of the step. If the binding curve is symmetrical, then the slope will also be symmetrical. This is shown to be the case for the particular situation found in Figure 1.

The changes in the optical density data in Figure 1 were converted into the fraction of sites occupied with CO by the use of eq 2. The fraction of sites occupied is given as $\theta(i)$

$$\theta(i) = \theta(0) - \frac{\sum_{j=1}^{i}\Delta OD(j)}{\Delta OD(\text{total})} \quad (2)$$

at the end of the ith step. The fraction of sites occupied at the beginning of the experiment, $\theta(0)$, where the pressure of CO is equal to the starting atmospheric pressure minus the vapor pressure of water, is computed by using the best-fit parameter, κ_{CO}, and is equal to 0.97 for the data in Figure 1. The measured change in optical density at the jth step is given as ΔOD(j), and the least-squares-fitted parameter representing the total change in optical density in going from a completely bound to a completely unbound state is given as ΔOD(total). The fraction of sites occupied is then used to produce a Hill plot (Hill, 1910). Note how well the data, when plotted in the Hill plot mode, fit the theoretical straight line expected for independent identical-site binding. The high precision of the data is also revealed by this plot.

The sensitivity of the Cary 219 instrument depends upon the particular scale range used. With a range of 1 OD, one typically finds that at least 0.001 OD change can be measured. Likewise, on a 0.1 OD range, at least 0.0001 change can be measured. Thus, low protein concentrations can be used without sacrificing precision. The lower the concentration, the more rapid the equilibration between the thin layer and the gas phase.

Results

Figure 1 illustrates typical CO binding data for *R. molischianum* ferrocytochrome *c'*. The data are given in terms of the observed change in optical density resulting from stepwise reductions in CO partial pressure as designated by a given step number. Binding data can be fit to a model which describes the shape of the binding curve in terms of a binding polynomial. The binding polynomial (Wyman, 1965), or what has been termed more recently the generating function (Hess & Szabo, 1979), is a summation of all specifically ligated macromolecular species in a system. The theoretical curve shown in Figure 1 was generated according to a binding model for two sites based on the assumption that each site binds CO

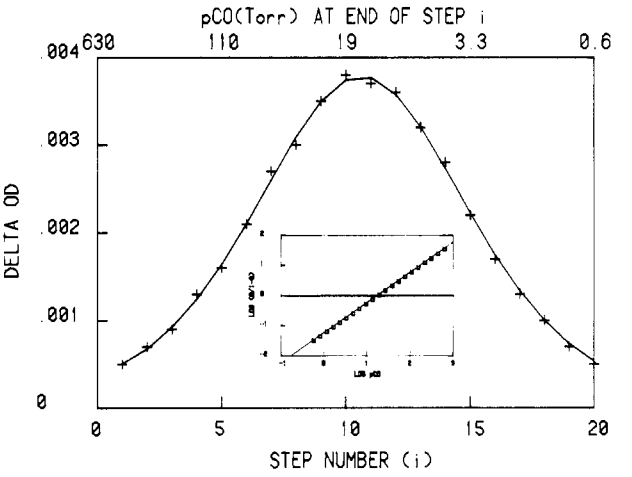

FIGURE 1: Actual data for carbon monoxide binding to *R. molischianum* ferrocytochrome *c'*. Experimental conditions were 0.1 M Tris, pH 7.3, 25 °C, and an atmospheric pressure of 630 torr. Changes in optical density are plotted against step number (i) [where the partial pressure of CO is changed from $p_{CO}(i-1)$ to $p_{CO}(i)$] along the lower abscissa. The corresponding partial pressure of CO at the end of a given step, $p_{CO}(i)$, is plotted along the upper abscissa. The solid curve is the theoretical single site binding function, generated with the fitted binding constant which is equal to 0.055 torr^{-1}. The data are represented as crosses, and the vertical lines of the crosses are equal to the standard error of the least-squares fit to the single site reaction equation. The inset displays the same data in the form of a Hill plot. The solid line with data points on it was generated with a single site binding equation using the same affinity constant of 0.055 torr^{-1}. The data were obtained directly from the ΔOD numbers in Figure 1 as described in the text. The horizontal line at log $[\theta/(1-\theta)] = 0$ goes through the theoretical curve at the half-saturation pressure (20 torr CO). The unit slope indicates that CO binds noncooperatively to *R. molischianum* ferrocytochrome *c'*.

with the same intrinsic binding constant, κ_{CO}. The binding polynomial, P_1, for this situation is

$$P_1 = (1+\kappa_{CO}p_{CO})(1+\kappa_{CO}p_{CO}) \quad (3)$$

The moles of ligand bound per mole of macromolecule, $\bar{X}$, is given by the partial derivative of the logarithm of the binding polynomial with respect to the logarithm of the partial pressure of ligand, p_{CO}, as (Wyman, 1948)

$$\bar{X} = \frac{\partial \ln P_1}{\partial \ln p_{CO}} = \frac{2\kappa_{CO}p_{CO}}{1+\kappa_{CO}p_{CO}} \quad (4)$$

The fraction of sites bound with CO, θ, is equal to $\bar{X}/2$ for a two-site molecule. The optical density change for a given stepwise dilution in CO partial pressure may be computed from the difference in θ for the two values of partial pressure times the parameter representing the total optical density change for complete ligation. The theoretical line shown in Figure 1 was generated by using a nonlinear least-squares fitting procedure (Bevington, 1969) which enables evaluation of the parameters of the model as well as an estimate of their standard errors (see Materials and Methods). An important criterion in testing the suitability of a given model is the comparison of the standard deviation of the fitted data with an independent estimate of the experimental error of the measuring instrument. The data were collected as changes in optical density. The experimental error in this measurement is about ±0.0001 optical density unit. Thus, if the magnitude of the standard deviation of the fitted data is comparable to this value, we conclude the model describes the system adequately. The error in the fit is equal to ±0.00005 optical density unit and agrees well with the error in the experimental measurements. Attempts to fit the data with more than one binding constant did not improve the fit. From the analysis

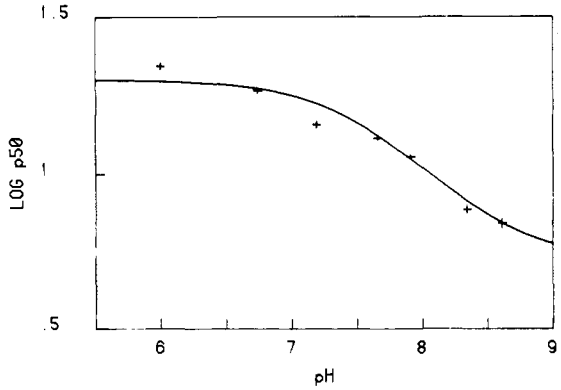

FIGURE 2: pH dependence of the log p_{50} (CO in torr) to *R. molischianum* ferrocytochrome *c′*. Data are represented as crosses with vertical lines of lengths equal to the standard error for determination of each particular log p_{50} value. The data, fitted to eq 6, give a standard deviation for a point equal to $\sigma = \pm 0.028$, $K_{H^+} = (2 \times 10^8) \pm (1 \times 10^8)$ M^{-1}, $K_{H^+,CO} = (6 \times 10^7) \pm (2 \times 10^7)$ M^{-1}, and log $p_{50}^0 = 0.7 \pm 0.1$.

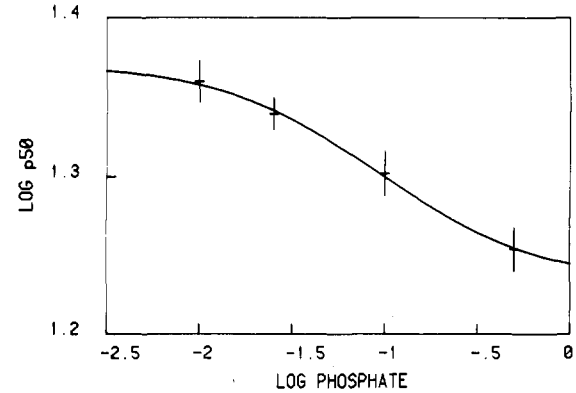

FIGURE 3: Phosphate dependence of log p_{50} (CO in torr) to *R. molischianum* ferrocytochrome *c′*. Data are represented as crosses with vertical lengths equal to the standard error for determination of each particular log p_{50} value. The data, fitted to eq 7, give a standard deviation for a point equal to $\sigma = \pm 0.0038$, $K_{phos} = 9 \pm 3$ M^{-1}, $K_{phos,CO} = 13 \pm 3$ M^{-1}, and log $p_{50}^0 = 1.371 \pm 0.006$.

of these particular results, as well as similar examination of all other CO binding experiments with this protein, we find that CO binding to *R. molischianum* ferrocytochrome *c′* involves sites which function independently and with identical CO affinity. The Hill plot in the inset of Figure 1 illustrates, by the observed straight line of unit slope, that the binding is noncooperative.

The effect of pH on the single binding constant, or p_{50} values, is shown in Figure 2. The number of protons displaced upon CO binding, or the magnitude of the Bohr effect, is given by the relationship (Antonini & Brunori, 1971):

$$\frac{d \log p_{50}}{d\ pH} = \bar{H}^+_{CO} - \bar{H}^+ = \Delta\bar{H}^+ \qquad (5)$$

where $\bar{H}^+_{CO}$ and $\bar{H}^+$ are the moles of protons bound per mole of CO binding site to the CO-bound and unligated cytochrome, respectively. The change in the number of protons bound per mole of CO, $\Delta\bar{H}^+$, is obtained from the slope of a log p_{50} vs. pH plot. The value of $\Delta\bar{H}^+$ determined at pH 8 equals -0.31 ± 0.04. The affinity for CO therefore increases with an increase in pH. The shape of the curve in Figure 2 is governed by proton binding groups which are linked to the CO binding process. This dependence can be expressed conveniently in terms of the pertinent proton binding polynomials (Wyman, 1948). The proton binding polynomials contain proton binding groups which are linked to CO ligation. Equation 6 shows

$$\log p_{50} = \log p_{50}^0 + \log\left(\frac{1 + K_{H^+}[H^+]}{1 + K_{H^+,CO}[H^+]}\right) \qquad (6)$$

this relationship in terms of half-saturation pressures for the case where only one proton ionizable group is linked to CO ligation. The CO half-saturation pressure at high pH is given as p_{50}^0. The proton binding constants for the CO-linked basic group in the unligated and CO-bound cytochrome are represented as K_{H^+} and $K_{H^+,CO}$, respectively. The theoretical curve in Figure 2 was generated from the least-squares fit values of $K_{H^+} = (2 \times 10^8) \pm (1 \times 10^8)$ M^{-1} and $K_{H^+,CO} = (6 \times 10^7) \pm (2 \times 10^7)$ M^{-1}. This represents a shift in the pK of the Bohr group from 8.3 in the unligated state to 7.8 in the CO-bound state.

The phosphate dependence of CO affinity is represented in Figure 3. The data were fitted to an equation similar to eq 6, only phosphate binding polynomials were substituted into the last term instead of proton binding polynomials. For the case where only one phosphate binding group is linked to the

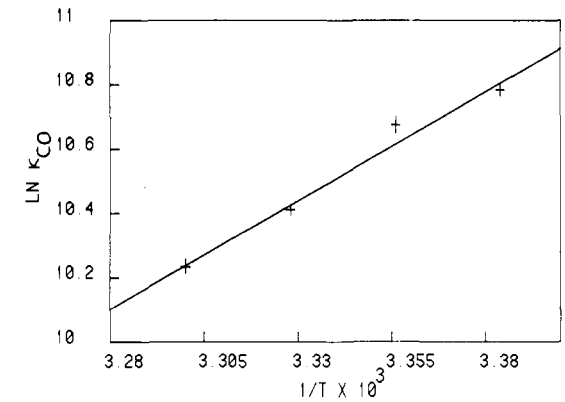

FIGURE 4: Temperature dependence of CO affinity to *R. molischianum* ferrocytochrome *c′*. The data are shown as crosses with vertical lines of length equal to the standard error for determination of each particular log p_{50} value. The data, fitted to the van't Hoff equation, give a heat of reaction of -10.7 kcal/mol of CO(aq) with a standard error of ± 1.2 kcal/mol.

CO binding reaction, the phosphate dependence on the logarithm of p_{50} can be described by

$$\log p_{50} = \log p_{50}^0 + \log\left(\frac{1 + K_{phos}[\text{phosphate}]}{1 + K_{phos,CO}[\text{phosphate}]}\right) \qquad (7)$$

where K_{phos} is the linked phosphate binding constant in the absence of CO and $K_{phos,CO}$ is the linked phosphate binding constant when the protein is ligated with CO. The half-saturation pressure of CO at zero concentration of phosphate is given as p_{50}^0. By least-squares analysis of the data in Figure 3, we find $K_{phos} = 9 \pm 3$ M^{-1} and $K_{phos,CO} = 13 \pm 3$ M^{-1}. Thus, the phosphate binding site which is linked to CO binding is half-saturated at 0.11 M phosphate in the reduced cytochrome and half-saturated at 0.08 M phosphate in the CO-bound form. The slope of the curve in Figure 3 yields the number of phosphate ions which are bound upon binding each CO molecule and is equal to 0.063 ± 0.003. The phosphate binding studies were done at pH 7.4. Since phosphate undergoes protonation at this pH, the linked function constants, K_{phos} and $K_{phos,CO}$, represent the reaction constant for the sum of all species of phosphate at that pH value.

The effect of temperature on the equilibrium constant κ_{CO} (i.e., p_{50}^{-1}) is shown for the values plotted in Figure 4 according to the van't Hoff equation. The heat of reaction determined from the slope is equal to -13.4 ± 1.2 kcal/mol of CO(g) which represents the heat of CO binding from the gas (g) phase. This includes the heat of solution of CO which is equal

to −2.7 kcal/mol of CO (Wilhelm et al., 1977). The heat of reaction from the liquid phase is then equal to −10.7 ± 1.2 kcal/mol of CO(aq). The observed heat of the reaction is similar to values reported for CO binding to hemoglobin and myoglobin (Antonini & Brunori, 1971).

Discussion

Equilibrium measurements show half-saturation values of about 20 torr CO (25 μM CO in water) for the binding of CO to *R. molischianum* ferrocytochrome *c'* at neutral pH. The measured affinity is consistent with CO affinities reported for other ferrocytochrome *c'* molecules (Cusanovich & Gibson, 1973) but is much lower than the affinity of CO for the globins (Antonini & Brunori, 1971). Comparison of the *R. molischianum* cytochrome *c'* structure to the globin structures shows unrelated tertiary structures, as well as major differences in the heme environment. Some of these structural differences may account for the intrinsic lower CO affinities in cytochrome *c'* relative to the globins. For example, residues in the ligand binding pocket of *R. molischianum* cytochrome *c'* are more tightly packed and more hydrophobic in character than those in the globin ligand pocket (Weber et al., 1981). Both structural features of cytochrome *c'* might contribute to reduced CO affinity due to steric crowding of the ligand and lack of a stabilizing hydrogen bond to the liganded CO.

The observed lack of cooperativity (see inset, Figure 1) for CO binding to the dimeric molecule *R. molischianum* ferrocytochrome *c'* indicates that CO ligation to each subunit involves only small structural changes. Thus, allosteric change in the quaternary structure of this molecule is probably minimal. Another interpretation of this observation is that the subunits have interfacial interactions which are insensitive to the state of ligation. This does not rule out linked effects with protons but does lead to the suggestion that these effects are due to localized changes, most likely in close proximity to the heme binding site.

Carbon monoxide affinity in heme proteins is affected by changes at the fifth axial ligand to the heme iron. In the globins, for example, the histidine axial ligand is buried in the hydrophobic protein interior with its Nd1 nitrogen hydrogen bonded to a backbone carbonyl oxygen (Valentine et al., 1979). Changes in hydrogen bonding to this histidine can influence CO affinity by regulating its ligand field strength and the strength of the heme iron–histidine nitrogen bond (Valentine et al., 1979; Peisach, 1975). In *R. molischianum* cytochrome *c'*, the histidine axial ligand and part of the heme group itself are exposed to solvent (Weber, 1982). As a result, the histidine lacks a hydrogen bond to the protein and is situated in a solvent-defined environment which is then sensitive to such factors as pH and phosphate concentration, as seen in our experimental data.

The affinity for carbon monoxide is found to increase with pH (see Figure 2). A large Bohr effect is observed and appears to be caused by a basic group whose pK is shifted from 8.3 in the unligated state to 7.8 in the CO-bound state. We feel that deprotonation of the axial histidine Nd1 proton controls the CO Bohr effect. Structural features of *R. molischianum* cytochrome *c'* which support this mechanism include the following: (1) free tyrosine, cysteine, or histidine side chains are absent; (2) the amino terminus is sufficiently removed from the heme that its pK is unlikely to change on ligand binding; and (3) both the histidine axial ligand and part of the corresponding heme face are exposed to solvent. Experimental data with model compounds and other heme proteins indicate that the pK for an axial histidine Nd1 proton is in the pH 9–10 range (Weber, 1982). In addition, NMR studies with *Rhodopseudomonas palustris* ferricytochrome *c'* implicate deprotonation of the fifth axial histidine at about pH 8 as a mechanism to control its heme physical properties (Jackson et al., 1983).

The affinity for CO is found to vary slightly with phosphate concentration. We feel this is probably due to phosphate binding at the histidine group or in its near environment. In the structure determination of *R. molischianum* cytochrome *c'*, a negatively charged mercury triiodide ion specifically complexed with the exposed heme face (Weber et al., 1981). The heavy metal–protein complex was stabilized by van der Waals contacts with adjacent protein atoms and electrostatic interactions with nearby positively charged amino acid side chains. Negatively charged ions such as hydroxide and phosphate might be similarly attracted to this region of the protein. A local concentration of ions at this site would increase the dielectric constant near the prosthetic group and alter the electronic distribution of the heme and its histidine axial ligand. Any rearrangement of heme electrons would be expected to alter ligand affinity at the sixth axial site.

The observed lack of cooperativity for CO binding and the marked heterotropic effects of protons and phosphate on the CO binding curve are consistent with the idea that significant allosteric structural changes are absent in this molecule and that localized structural changes near the heme control CO ligation at the heme site. Most likely, this occurs at the histidine axial ligand. The solvent-exposed environment of the histidine axial ligand provides the opportunity to study directly its influence on the functional properties of histidine-liganded heme proteins. The direct access of solvent to the histidine ligand in cytochrome *c'* requires close monitoring of the buffer systems used. For example, it has been previously noted that the Mössbauer spectra of cytochrome *c'* are buffer dependent at neutral pH (Emptage et al., 1981). Therefore, carefully controlled studies on the cytochromes *c'* are important toward understanding the unique properties of these proteins and their relationship to other proteins.

Acknowledgments

We thank Dr. Michael A. Cusanovich for kindly providing the protein samples used in this study.

Registry No. CO, 630-08-0; cytochrome *c'*, 9035-41-0; phosphate, 14265-44-2.

References

Antonini, E., & Brunori, M. (1971) in *Hemoglobin and Myoglobin in Their Reactions with Ligands* (Neuberger, A., & Tatum, E. L., Eds.) North-Holland, Amsterdam.

Bartsch, R. G. (1971) *Methods Enzymol. 23*, 344–363.

Bartsch, R. G. (1978) in *The Photosynthetic Bacteria* (Clayton, R. K., & Sistrom, W. R., Eds.) pp 249–280, Plenum Press, New York.

Bevington, P. R. (1969) in *Data Reduction and Error Analysis for the Physical Sciences*, McGraw-Hill, New York.

Cusanovich, M. A., & Gibson, Q. H. (1973) *J. Biol. Chem. 248*, 822–834.

Dolman, D., & Gill, S. J. (1978) *Anal. Biochem. 87*, 127–134.

Emptage, M. H., Xavier, A. V., Wood, J. M., Alsaadi, B. M., Moore, G. R., Pitt, R. C., Williams, R. J. P., Ambler, R. P., & Bartsch, R. G. (1981) *Biochemistry 20*, 58–64.

Hayashi, A., Suzuki, T., & Shin, M. (1973) *Biochim. Biophys. Acta 310*, 309–316.

Hess, V. L., & Szabo, A. (1979) *J. Chem. Educ. 56*, 289.

Hill, A. V. (1910) *J. Physiol. (London) 40*, iv–vii.

Jackson, J. T., La Mar, G. N., & Bartsch, R. G. (1983) *J. Biol. Chem. 258*, 1799–1805.

Peisach, J. (1975) *Ann. N.Y. Acad. Sci. 244*, 187–203.
Rubinow, S. C., & Kassner, R. J. (1984) *Biochemistry 23*, 2590–2595.
Taniguchi, S., & Kamen, M. D. (1963) *Biochim. Biophys. Acta 74*, 438–455.
Valentine, J. S., Sheridan, R. P., Allen, L. C., & Kahn, P. C. (1979) *Proc. Natl. Acad. Sci. U.S.A. 76*, 1009–1013.
Weber, P. C. (1982) *Biochemistry 21*, 5116–5119.
Weber, P. C., Howard, A., Huu Xuong, N., & Salemme, F. R. (1981) *J. Mol. Biol. 153*, 399–424.
Wilhelm, E., Battino, R., & Wilcock, R. J. (1977) *Chem. Rev. 77*, 219–262.
Wyman, J. (1948) *Adv. Protein Chem. 4*, 407–531.
Wyman, J. (1965) *J. Mol. Biol. 11*, 631.

Substrate-Induced Modifications of the Intrinsic Fluorescence of the Isolated Adenine Nucleotide Carrier Protein: Demonstration of Distinct Conformational States

Gérard Brandolin,*,‡ Yves Dupont,§ and Pierre V. Vignais‡

Laboratoire de Biochimie (CNRS/ERA 903 et INSERM U.191), Département de Recherche Fondamentale, and Laboratoire de Biologie Moléculaire et Cellulaire, Département de Recherche Fondamentale, Centre d'Etudes Nucléaires, 38041 Grenoble Cedex, France

Received August 6, 1984

ABSTRACT: The effects of ATP or ADP and the specific inhibitors carboxyatractyloside (CATR) and bongkrekic acid (BA) on the conformation of the isolated adenine nucleotide (AdN) carrier protein were studied by fluorescence spectroscopy. The addition of ATP to the AdN carrier resulted in a rapid fluorescence increase of the tryptophanyl residue(s) at 355 nm, which leveled up in less than 1 s at 22 °C. Among the natural nucleotides, only ATP and ADP were effective. At 10 °C or below, the kinetics of the fluorescence increase induced by ATP were biphasic, consisting of a rapid phase of less than 1 s, followed by a slower phase that lasted for a few seconds and had virtually the same amplitude as the rapid one. Both phases were abolished when CATR was added prior to ATP or fully reversed when CATR was added after the fluorescence response to ATP had been elicited. The number of CATR binding sites present on the carrier protein was determined by CATR specific inhibition of the ATP-induced increase in intrinsic fluorescence. The calculated number of CATR sites was equal to that found by another method based on the use of the same preparation of AdN carrier loaded with fluorescent nucleotide naphthoyl-ATP and on the CATR-induced release of the bound naphthoyl-ATP, demonstrating the reliability of the intrinsic fluorescence assay. Addition of BA prior to or together with ATP nearly doubled the amplitude of the ATP-induced fluorescence signal. At 10 °C or below, the fluorescence response to ATP in the presence of BA could also be decomposed into rapid and slow phases. The amplitude of the rapid phase was not modified in the presence of BA, but in contrast to the fluorescence signal induced by ATP alone, the amplitude of the slow phase was about 3 times higher than that of the rapid phase. The same results were obtained when ATP was replaced by ADP. In the absence of ATP, CATR was found to induce per se a modification of the intrinsic fluorescence that differed from that induced by ATP by its excitation and emission spectra. These results are discussed on the basis of a minimal model where the AdN carrier is supposed to exist in two native conformations, the CATR and BA conformations that are trapped and stabilized by CATR and BA, respectively; interconversion between the two conformations is triggered by ATP or ADP. However, on the basis of several observations that point to a tetrameric organization of the AdN carrier protein, it is equally possible that the transition between the CATR and BA conformations is multiphasic and may proceed with sequential modification of each subunit of the tetramer.

The mitochondrial AdN carrier isolated in detergent and purified by hydroxylapatite chromatography is able to respond specifically to the addition of ADP or ATP by modification of its intrinsic fluorescence (Brandolin et al., 1981). The nucleotide-induced fluorescence signal was most likely due to changes in the environment of the tryptophanyl residue(s) caused by conformational changes resulting from the binding of nucleotides to the carrier protein. Carboxyatractyloside (CATR),[1] an inhibitor of AdN transport that reacts with the carrier on the outer face of the inner mitochondrial membrane, prevented the fluorescence increase when added prior to ADP or ATP and decreased it when added after the fluorescence rise had been initiated. On the other hand, bongkrekic acid (BA), another inhibitor that attacks the carrier from the inside

‡ Laboratoire de Biochimie, Centre d'Etudes Nucléaires.
§ Laboratoire de Biologie Moléculaire et Cellulaire, Centre d'Etudes Nucléaires.

[1] Abbreviations: AdN carrier, adenine nucleotide carrier; CATR, carboxyatractyloside; BA, bongkrekic acid; LAPAO, 3-lauramido-*N*,*N*-dimethylpropylamine oxide; N-ATP, naphthoyladenosine 5′-triphosphate; FTP, formycin triphosphate; Mops, 4-morpholinepropanesulfonic acid; EDTA, ethylenediaminetetraacetic acid.

0006-2960/85/0424-1991$01.50/0